華中師範大學
CENTRAL CHINA NORMAL UNIVERSITY

Multiprocess imaging of nuclear modifications on parton distributions in proton-nucleus collisions

Meng-Quan Yang

Collaborated with Peng Ru, Ben-Wei Zhang

M.~Q.~Yang, *P.~Ru and B.~W.~Zhang, Phys. Rev. D 112 (2025) no.7, 074008*

28/11/2025

Outline

- Introduction
- Imaging $r_i^A(x, Q^2)$ in pA collisions
- Summary

Introduction

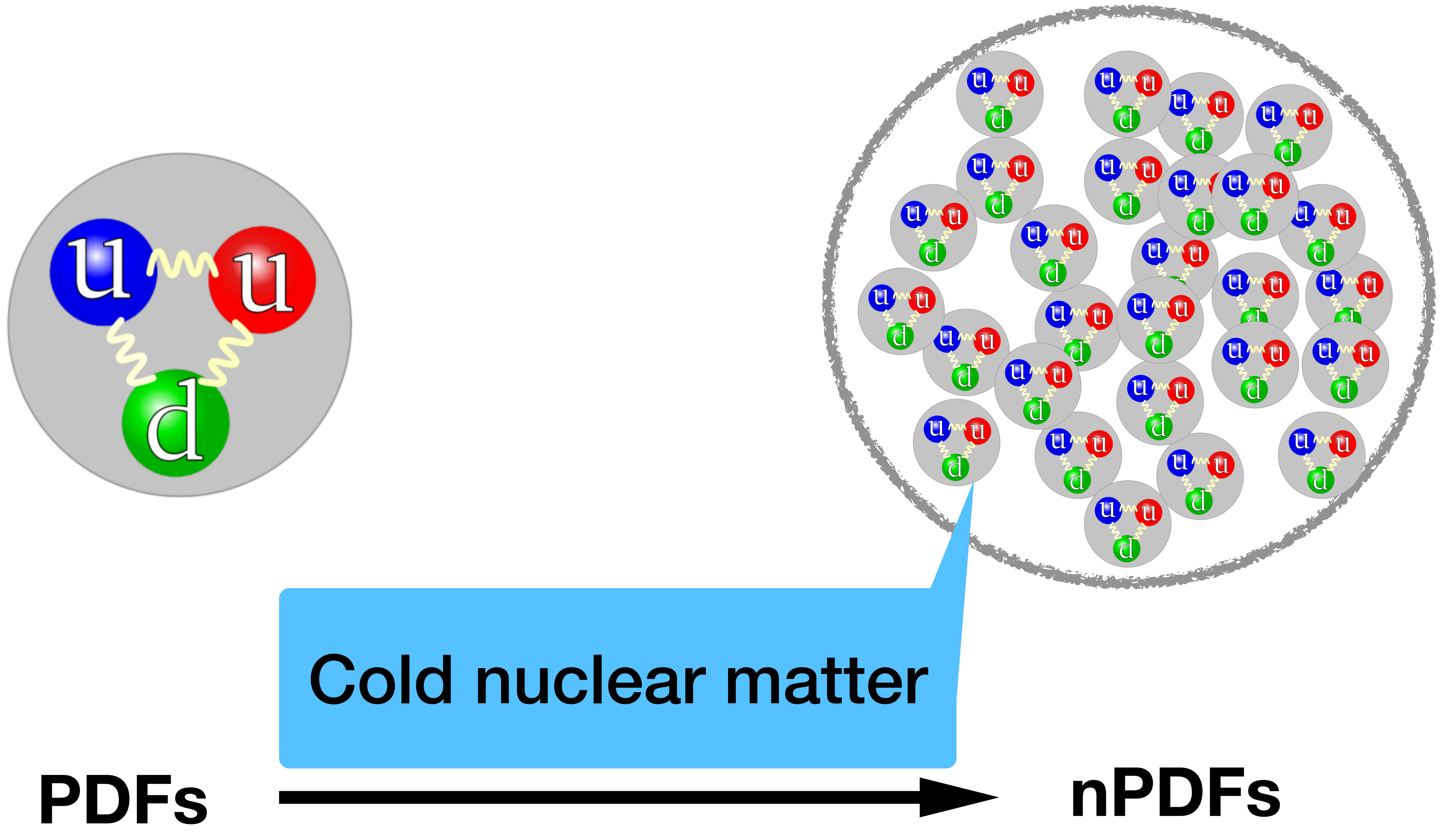

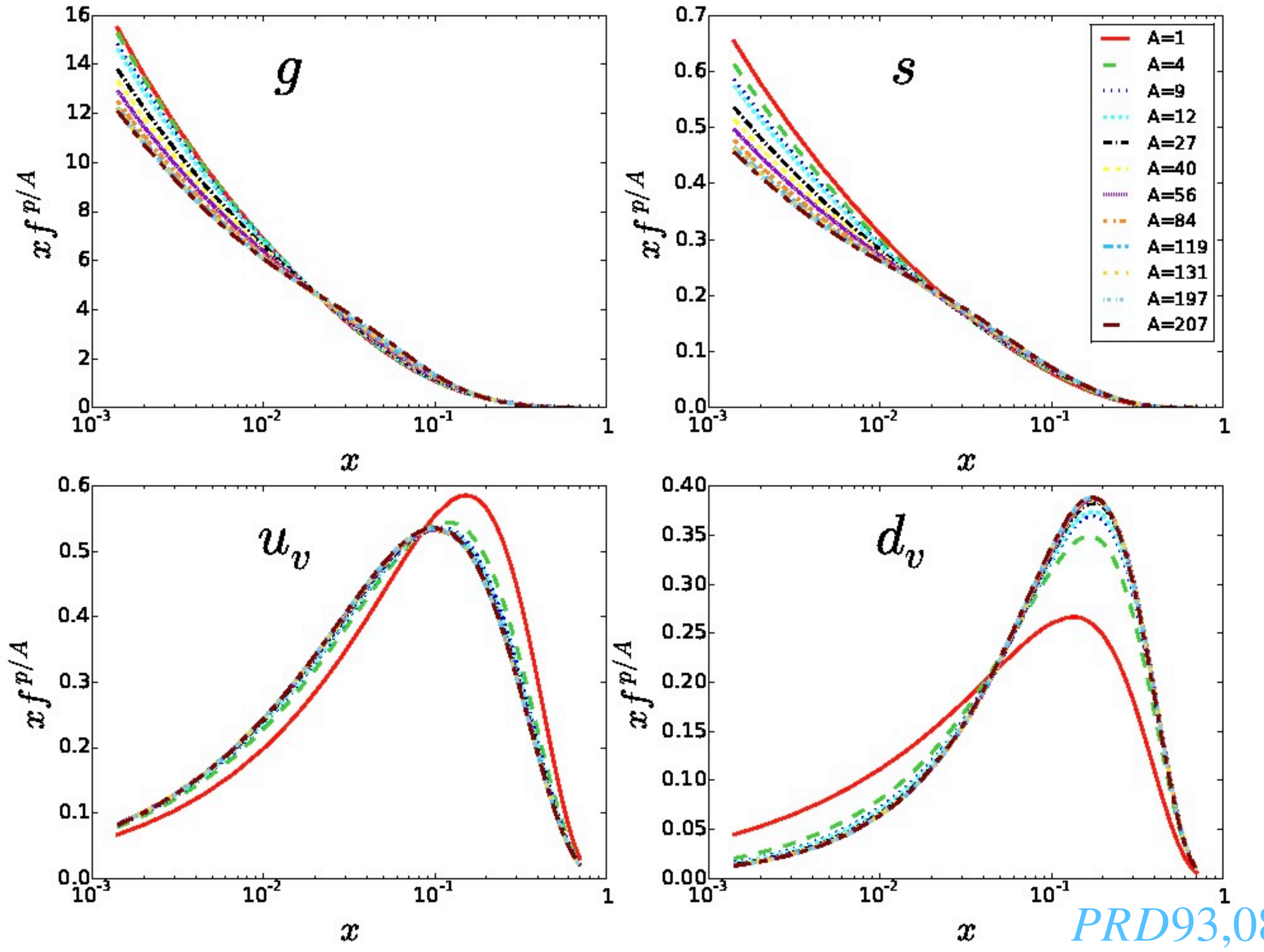

*PRD*93,085037(2016)

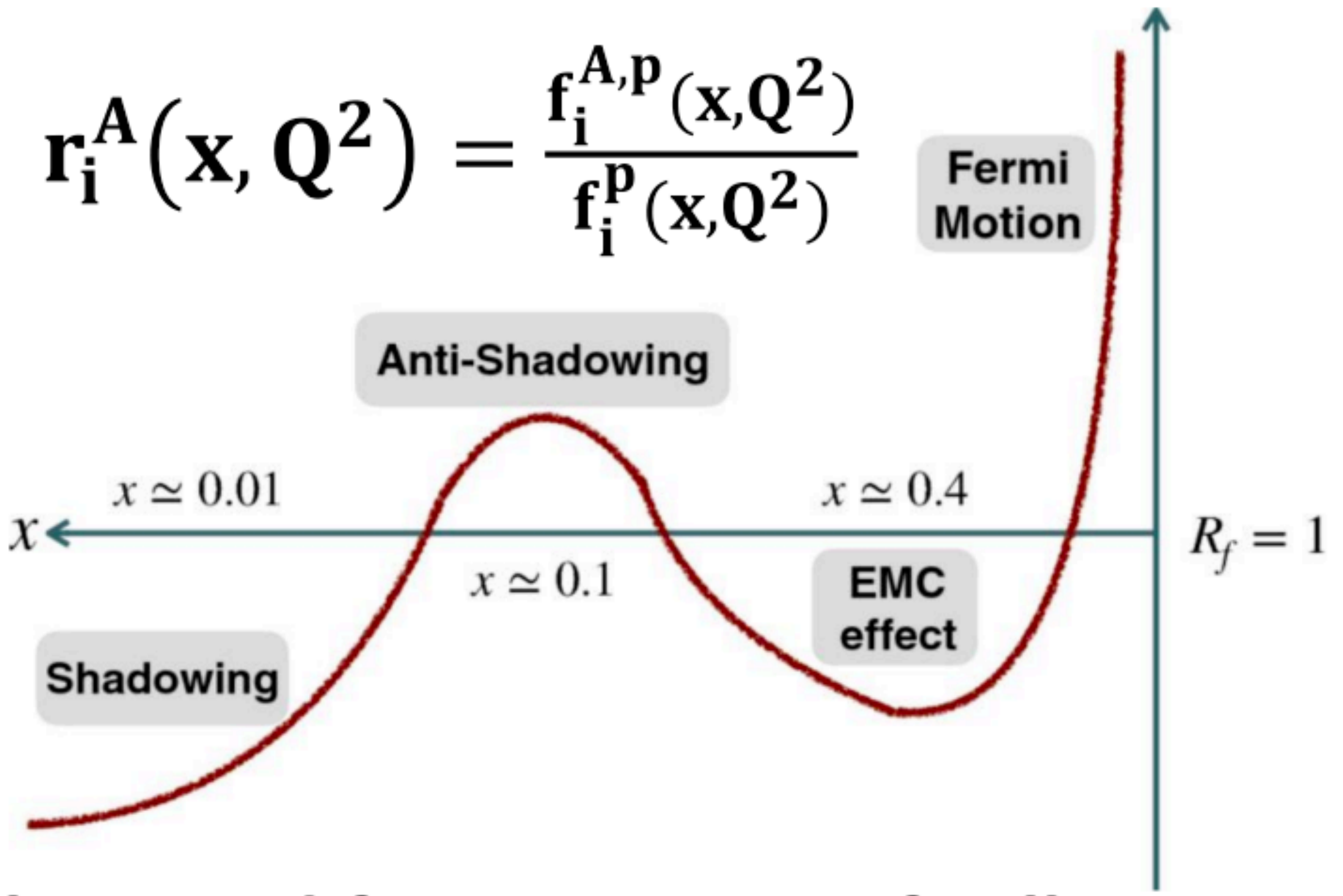

Nuclear modification ratios of collinear PDFs.

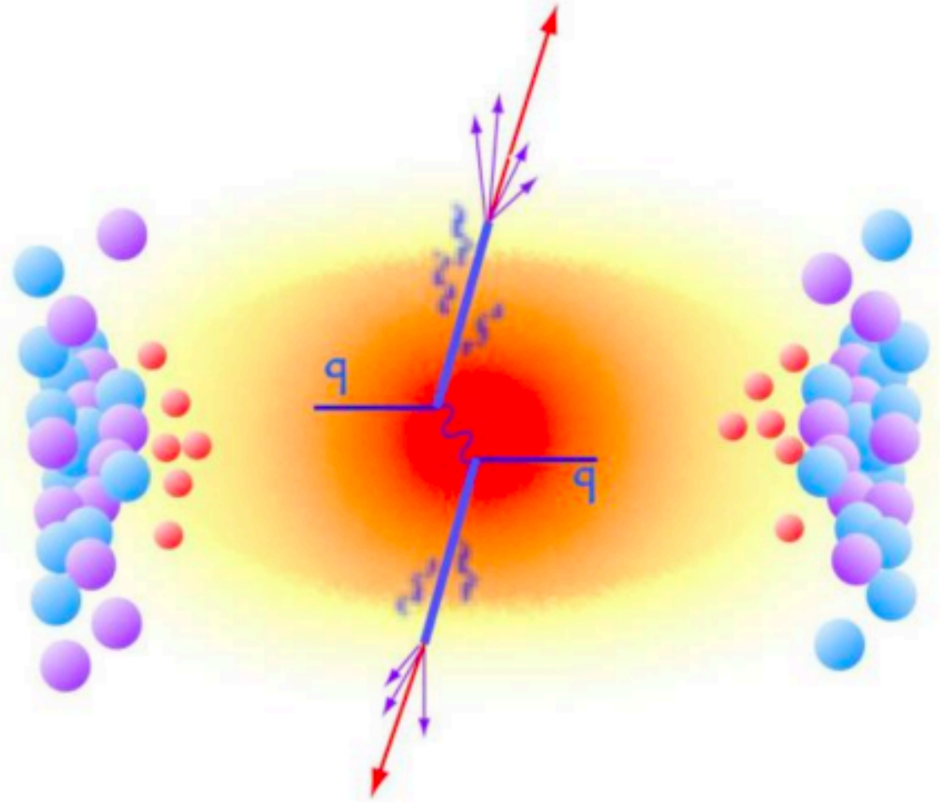

An essential baseline for disentangling final-state nuclear matter effects probed by hard particles.

Introduction

Eur. Phys. J. C (2017) 77:163

Table 1 The data sets used in the EPPS16 analysis, listed in the order of growing nuclear mass number. The number of data points and their contribution to χ^2 counts only those data points that fall within the kinematic cuts explained in the EPS09 analysis are marked with

Experiment	Observable	Collisions	Data points
SLAC E139	DIS	e^-He(4), e^-D	21
CERN NMC 95, re	DIS	μ^-He(4), μ^-D	16
CERN NMC 95	DIS	μ^-Li(6), μ^-D	15
CERN NMC 95, Q^2 dep	DIS	μ^-Li(6), μ^-D	153
SLAC E139	DIS	e^-Be(9), e^-D	20
CERN NMC 96	DIS	μ^-Be(9), μ^-C	15
SLAC E139	DIS	e^-C(12), e^-D	7
CERN NMC 95	DIS	μ^-C(12), μ^-D	15
CERN NMC 95, Q^2 dep	DIS	μ^-C(12), μ^-D	165
CERN NMC 95, re	DIS	μ^-C(12), μ^-D	16
CERN NMC 95, re	DIS	μ^-C(12), μ^-Li(6)	20
FNAL E772	DY	pC(12), pD	9
SLAC E139	DIS	e^-Al(27), e^-D	20
CERN NMC 96	DIS	μ^-Al(27), μ^-C(12)	15
SLAC E139	DIS	e^-Ca(40), e^-D	7
FNAL E772	DY	pCa(40), pD	9
CERN NMC 95, re	DIS	μ^-Ca(40), μ^-D	15
CERN NMC 95, re	DIS	μ^-Ca(40), μ^-Li(6)	20
CERN NMC 96	DIS	μ^-Ca(40), μ^-C(12)	15
SLAC E139	DIS	e^-Fe(56), e^-D	26
FNAL E772	DY	e^-Fe(56), e^-D	9
CERN NMC 96	DIS	μ^-Fe(56), μ^-C(12)	15
FNAL E866	DY	pFe(56), pBe(9)	28
CERN EMC	DIS	μ^-Cu(64), μ^-D	19
SLAC E139	DIS	e^-Ag(108), e^-D	7
CERN NMC 96	DIS	μ^-Sn(117), μ^-C(12)	15
CERN NMC 96, Q^2 dep	DIS	μ^-Sn(117), μ^-C(12)	144
FNAL E772	DY	pW(184), pD	9
FNAL E866	DY	pW(184), pBe(9)	28
CERN NA10[a]	DY	π^-W(184), π^-D	10
FNAL E615[a]	DY	π^+W(184), π^-W(184)	11
CERN NA3[a]	DY	π^-Pt(195), π^-H	7
SLAC E139	DIS	e^-Au(197), e^-D	21
RHIC PHENIX	π^0	dAu(197), pp	20
CERN NMC 96	DIS	μ^-Pb(207), μ^-C(12)	15
CERN CMS[a]	$W^\pm$	pPb(208)	10
CERN CMS[a]	Z	pPb(208)	6
CERN ATLAS[a]	Z	pPb(208)	7
CERN CMS[a]	dijet	pPb(208)	7
CERN CHORUS[a]	DIS	νPb(208), $\bar{\nu}$Pb(208)	824
Total			1811

Global QCD analysis

Both PDFs and their nuclear modification ratios rely on the global QCD analyses of diverse experimental data.

$$r_i^A(x, Q^2) = \frac{f_i^{A,p}(x, Q^2)}{f_i^p(x, Q^2)}$$

Challenge in global analyses:

For a realistic observable, the dependencies on x, Q^2, and i are intricately convoluted in calculations with collinear factorization in perturbative QCD.

$$d\sigma = \sum_{abd} f_{a/A}(x_a, \mu_F) \otimes f_{b/B}(x_b, \mu_F) \otimes d\hat{\sigma}_{ab\to cd}(x_a P_A, x_b P_B, \mu_F, \mu_R) \otimes D_{c\to h}(z_h, \mu_F)$$

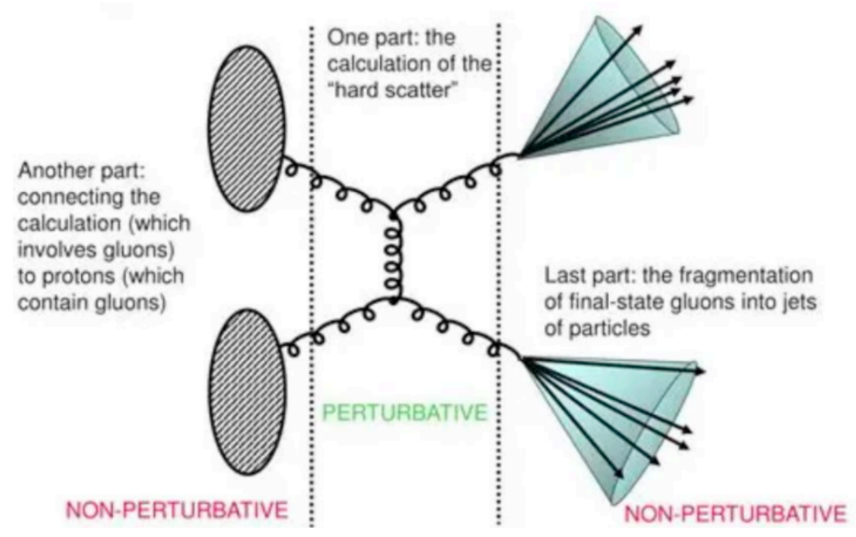

Introduction

Challenge in global analyses:
An analogy to solving a system of equations

$$\begin{cases} a_{11}x_1 + a_{12}x_2 + \cdots + a_{1n}x_n = O_1 \\ a_{21}x_1 + a_{22}x_2 + \cdots + a_{2n}x_n = O_2 \\ \vdots \\ \vdots \\ a_{n1}x_1 + a_{n2}x_2 + \cdots + a_{nn}x_n = O_n \end{cases}$$

$$\Downarrow$$

$$\{x_1, x_2, \cdots, x_n\}$$

Lower degree of variable mixing results in faster solving.

$$\begin{cases} a_{11}x_1 = O_1 \\ a_{21}x_1 + a_{22}x_2 = O_2 \\ \vdots \\ \vdots \\ a_{nn}x_n = O_n \end{cases}$$

$$\Downarrow$$

$$\{x_1, x_2, \cdots, x_n\}$$

Introduction

Challenge in global analyses:
An analogy to solving a system of equations

$$\begin{cases} a_{11}x_1 + a_{12}x_2 + \cdots + a_{1n}x_n = O_1 \\ a_{21}x_1 + a_{22}x_2 + \cdots + a_{2n}x_n = O_2 \\ \vdots \\ \vdots \\ a_{n1}x_1 + a_{n2}x_2 + \cdots + a_{nn}x_n = O_n \end{cases}$$

$$\{x_1, x_2, \cdots, x_n\}$$

Challenge from mixing contributions of variables
1. Overfitting.
2. Parameters degeneracy.
3. Complicated uncertainty propagation.
4. Slow and unstable convergence.

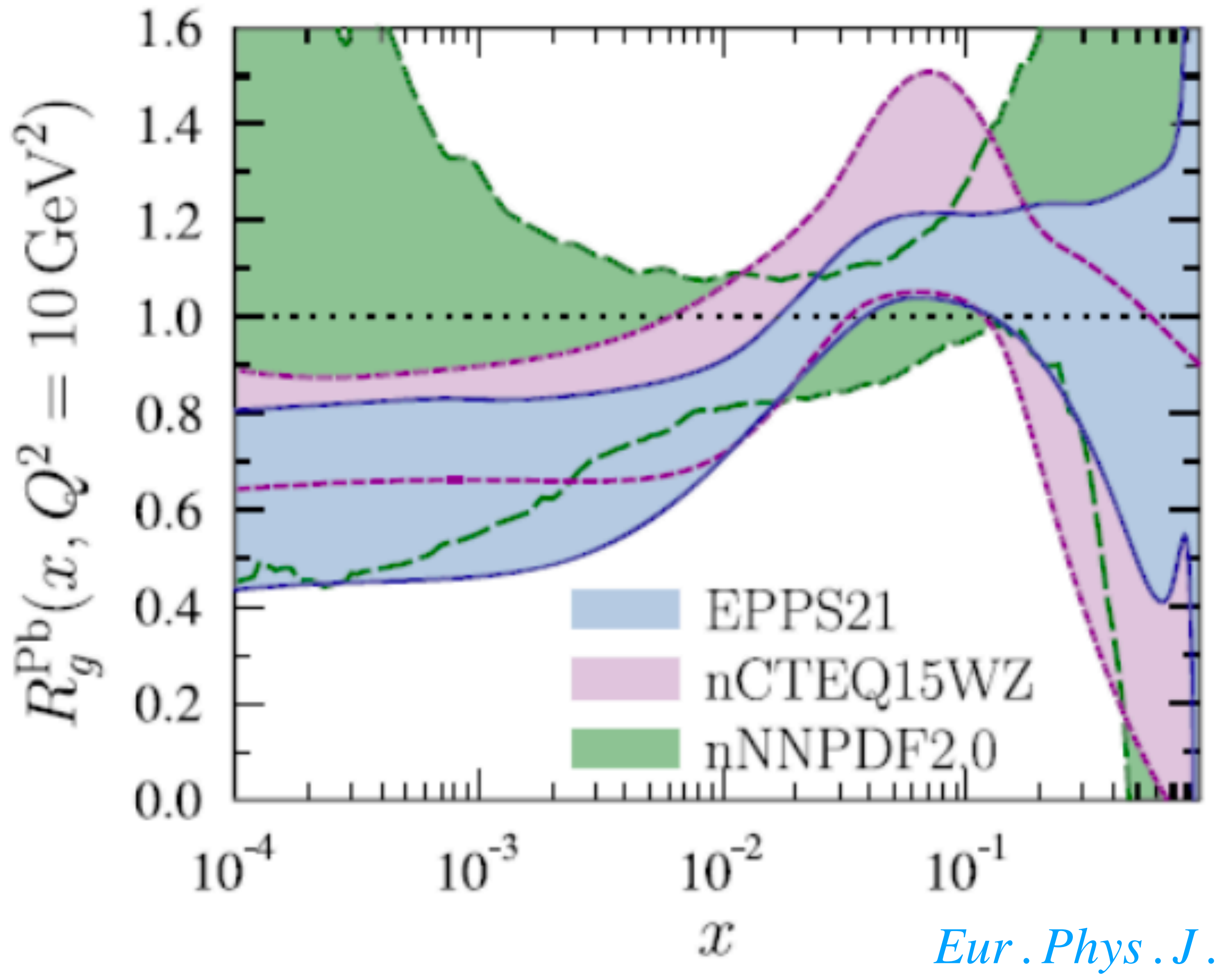

*Eur . Phys . J . C*82(2022)5,413

Introduction

Insights from nuclear binding dynamics are useful.

Short-Range Correlations

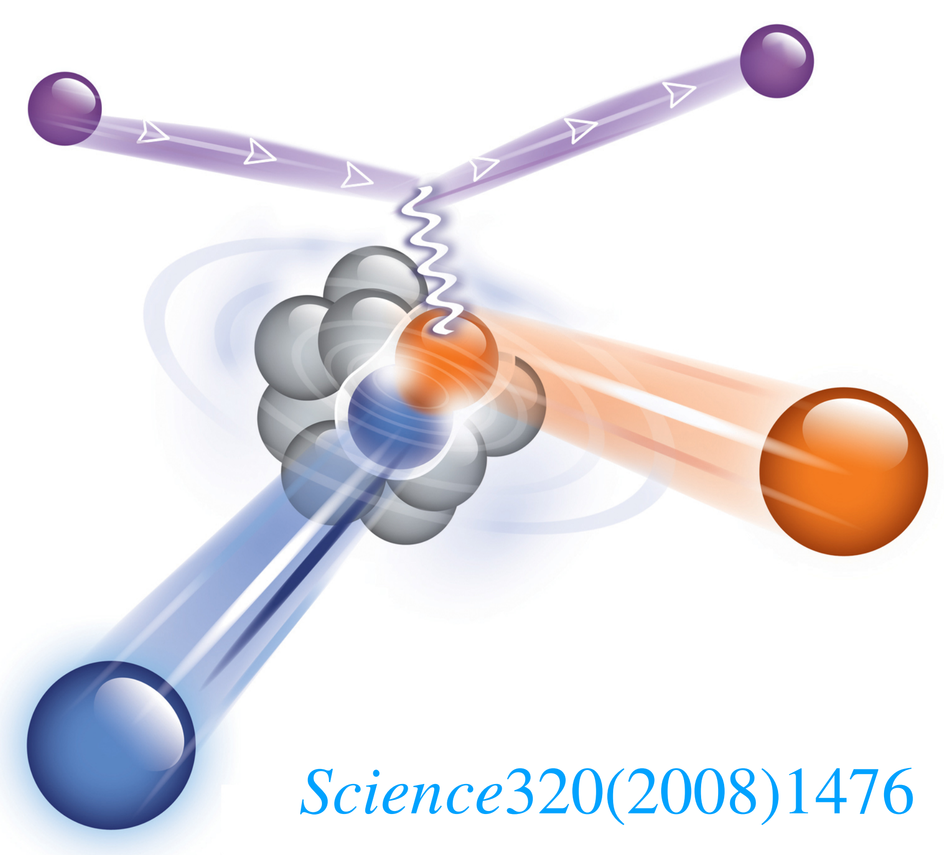

Science 320(2008)1476

Phys. Rev. Lett. 133(2024)15,152502

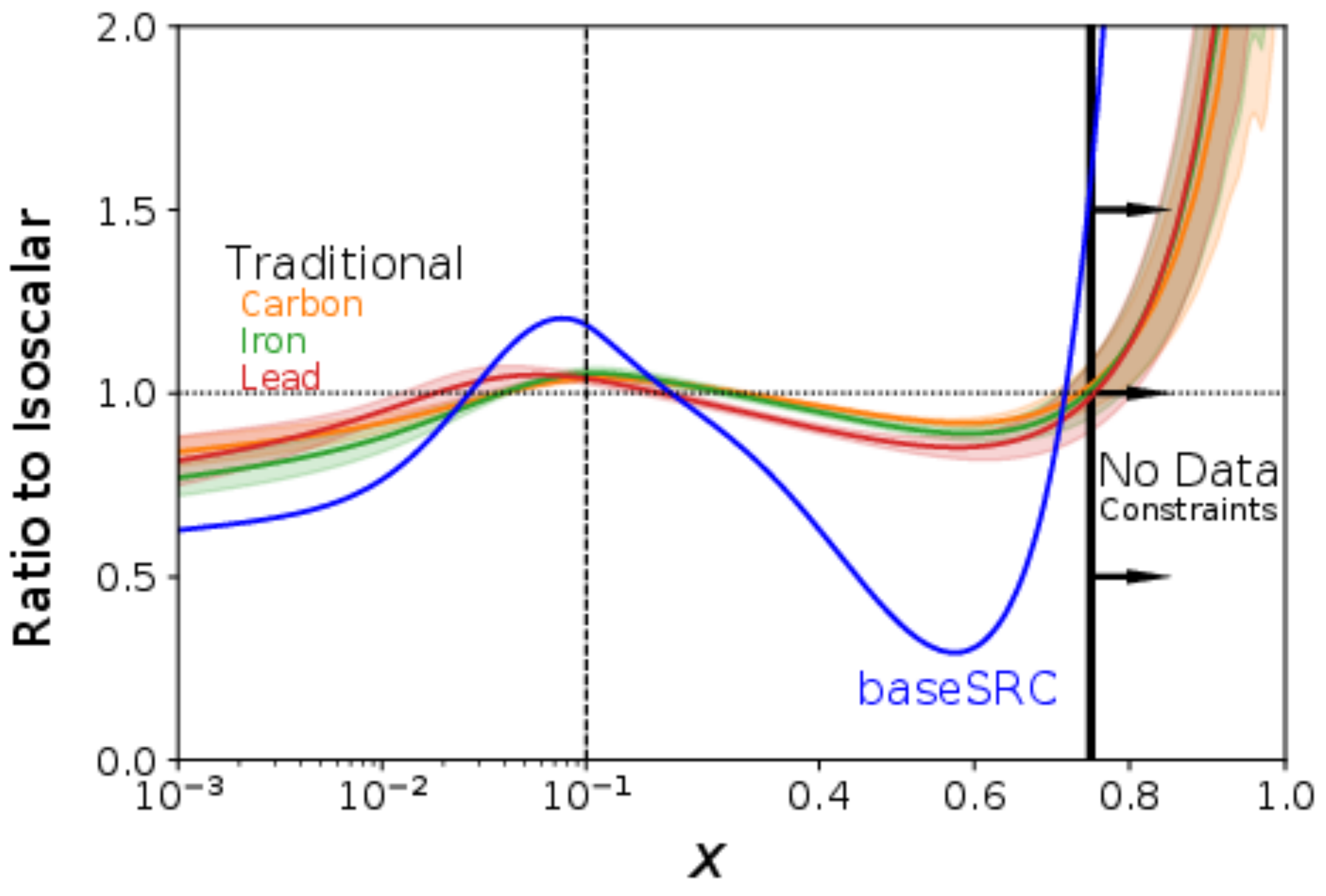

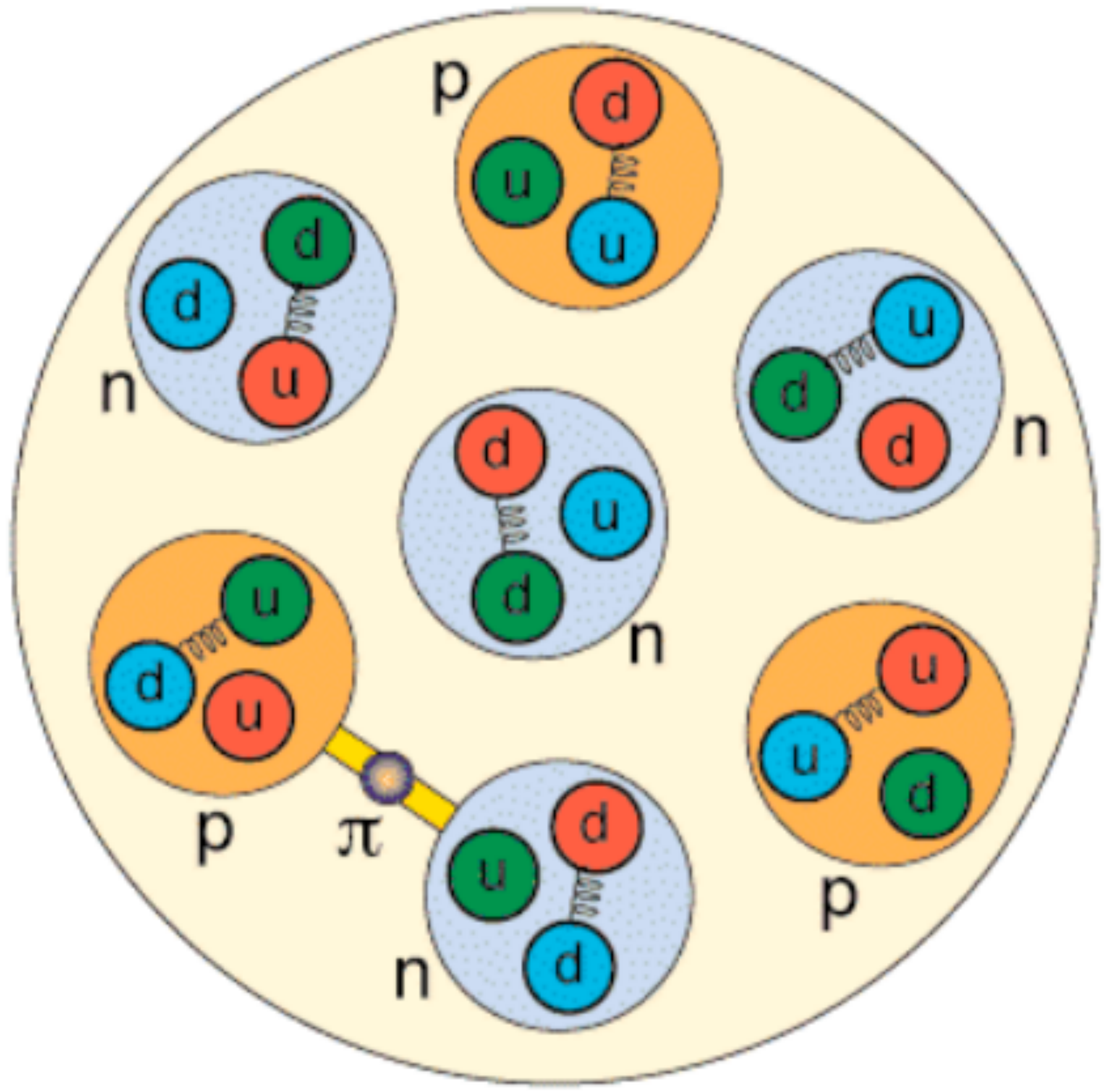

Meson exchange current
Off-shell corrections
Coherent nuclear shadowing
Fermi motion
……

Phys. Rev. C 90(2014)4,045204

Introduction

Data in DIS serve as an effective image of $r_i^A(x, Q^2)$

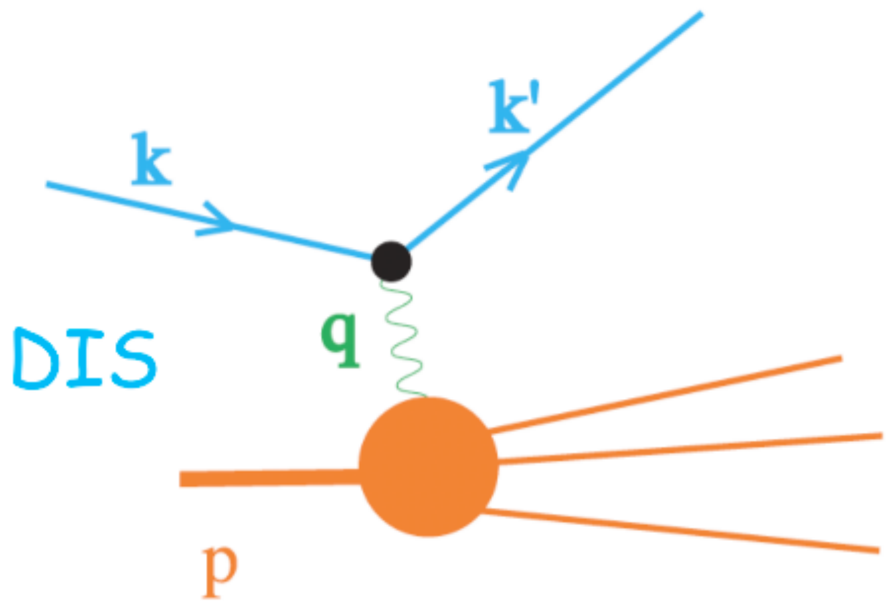

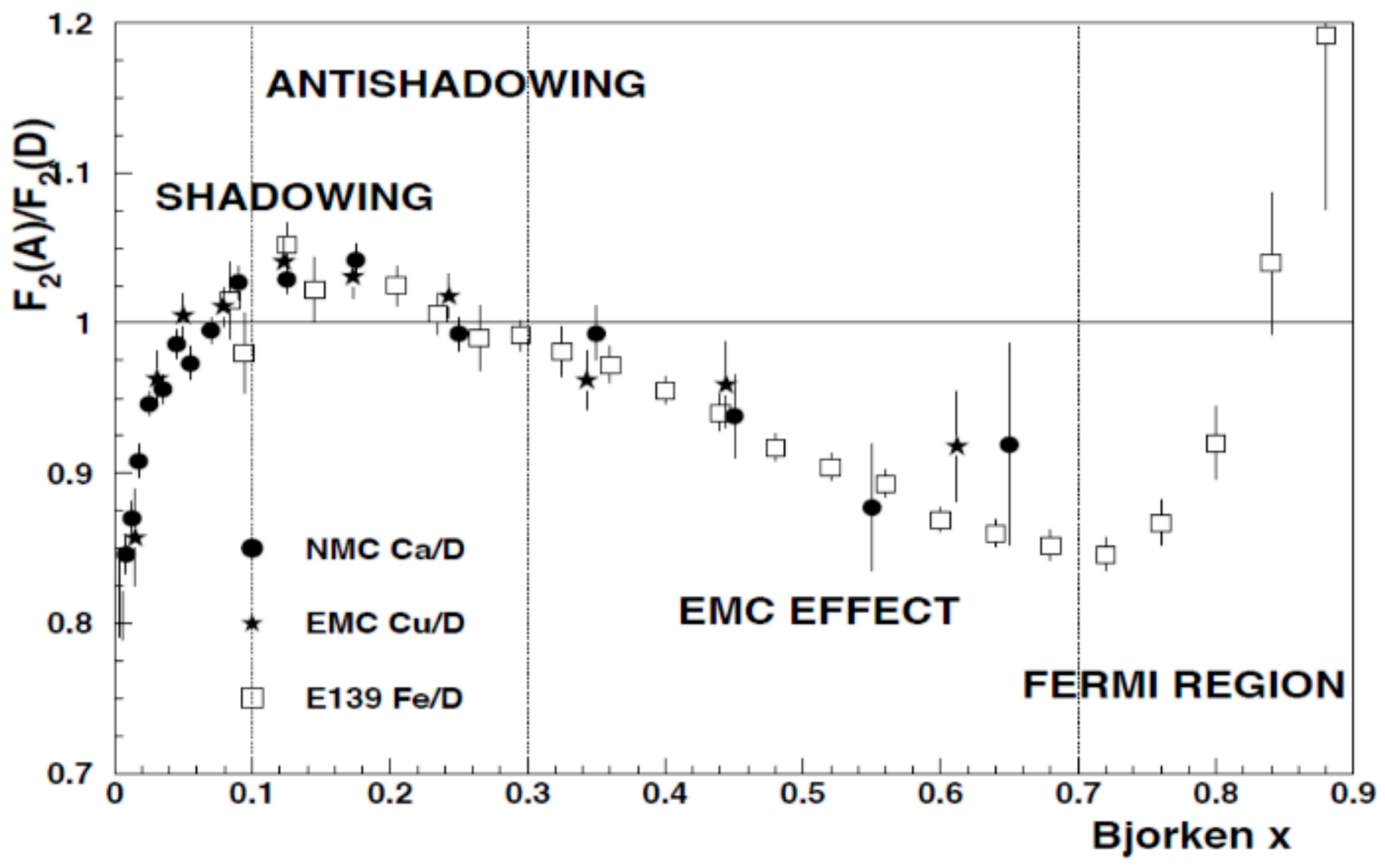

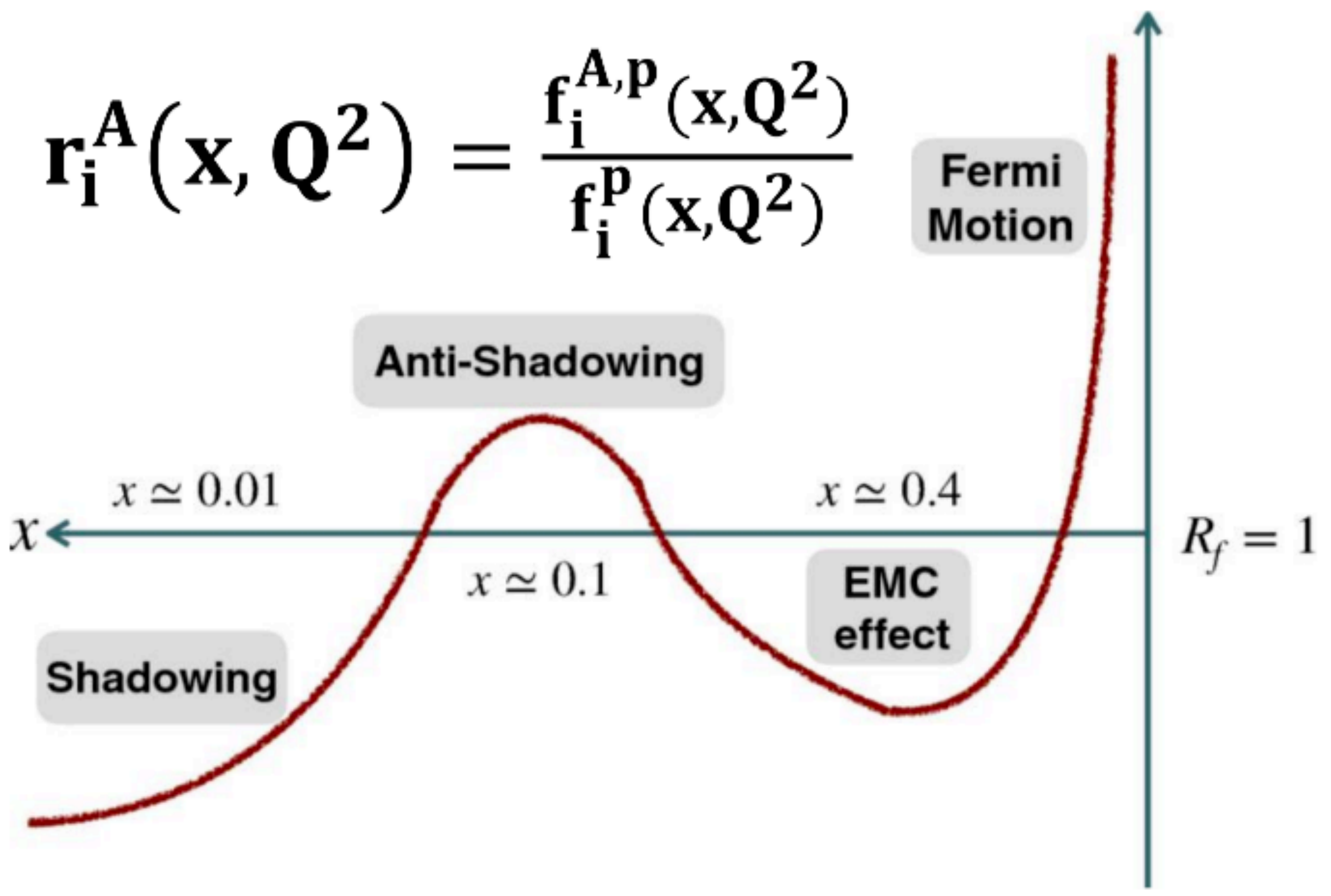

Measurement of such observable with low degree of variable mixing:

1. inspire parametrizations of modifications

2. improve the efficiency of global analysis.

Motivation

Status for pA collisions at the LHC

Phys. Rev. Lett. 131(2023)4,042302

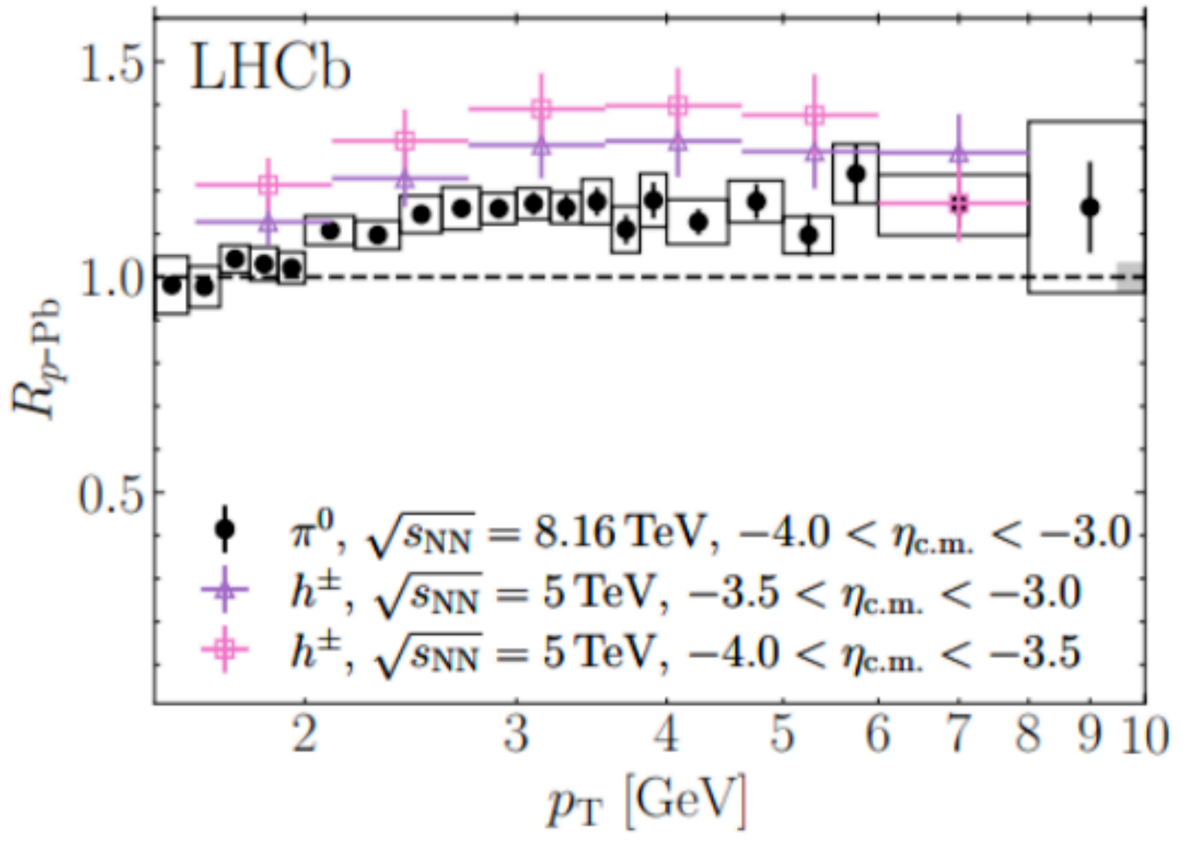

JHEP 06(2015),055

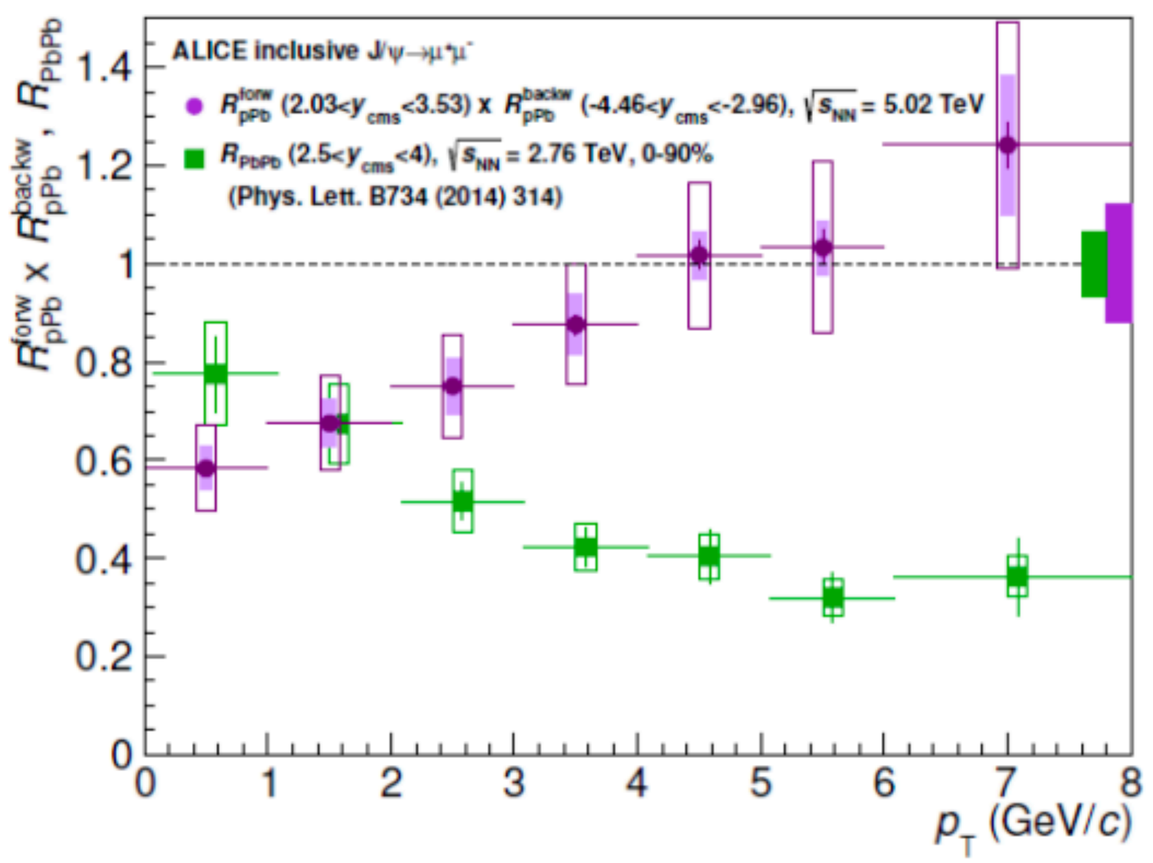

Phys. Rev. Lett. 121(2018)6,062002

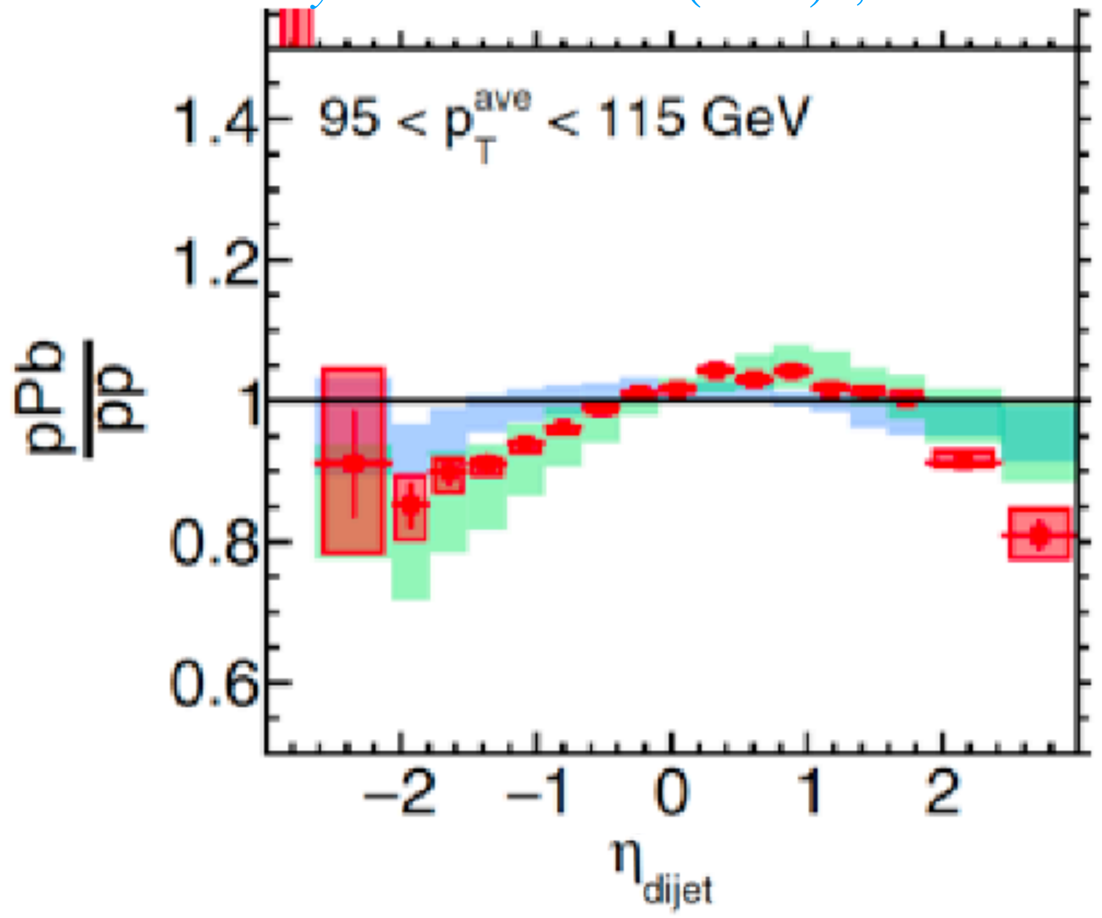

Phys. Lett. B 800(2020),135048

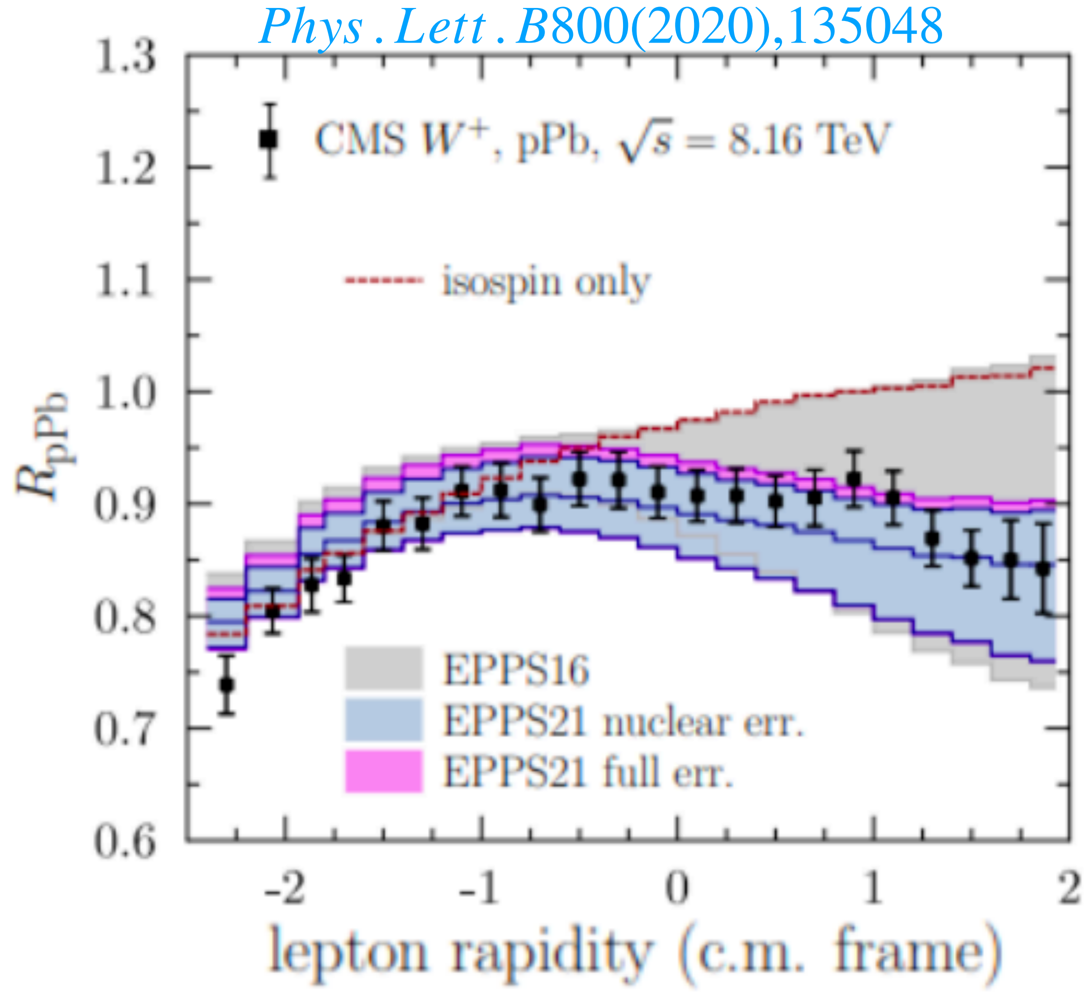

However, the imaging of $r_i^A(x, Q^2)$ achieved in DIS has not been replicated for most LHC processes.

Can we image $r_i^A(x, Q^2)$ at LHC?

Construction of the image of $r_i^A(x, Q^2)$ in pA

Triple differential dijet cross section

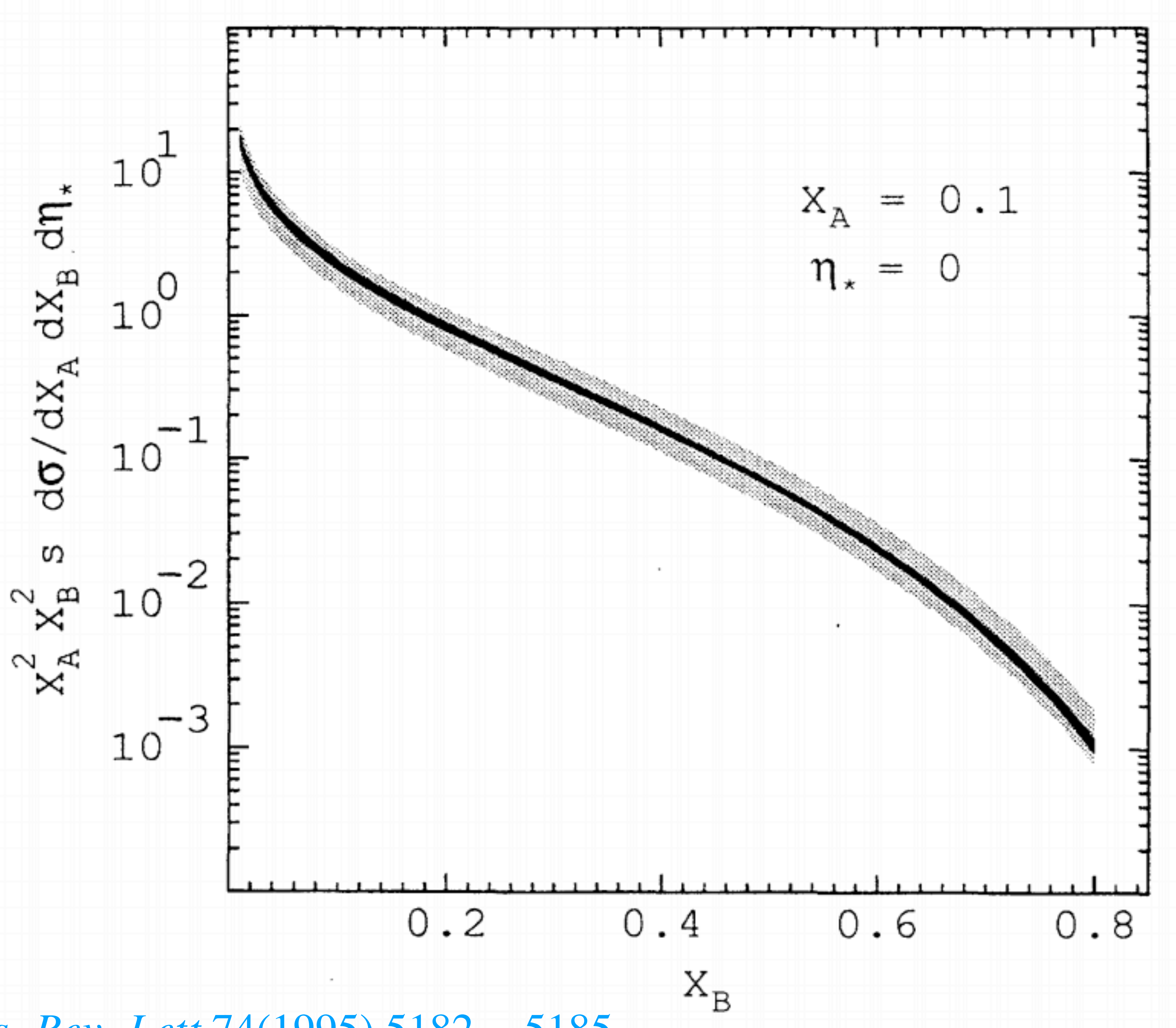

*Phys . Rev . Lett.*74(1995),5182 – 5185

$$V^{(3)} = \{X_B, X_A, y^*\}$$

$$X_A = \sum_{n\in\text{dijets}} \frac{E_{Tn}}{\sqrt{s}} e^{+y_n}$$

$$X_B = \sum_{n\in\text{dijets}} \frac{E_{Tn}}{\sqrt{s}} e^{-y_n}$$

*PRD*105,096025(2022)

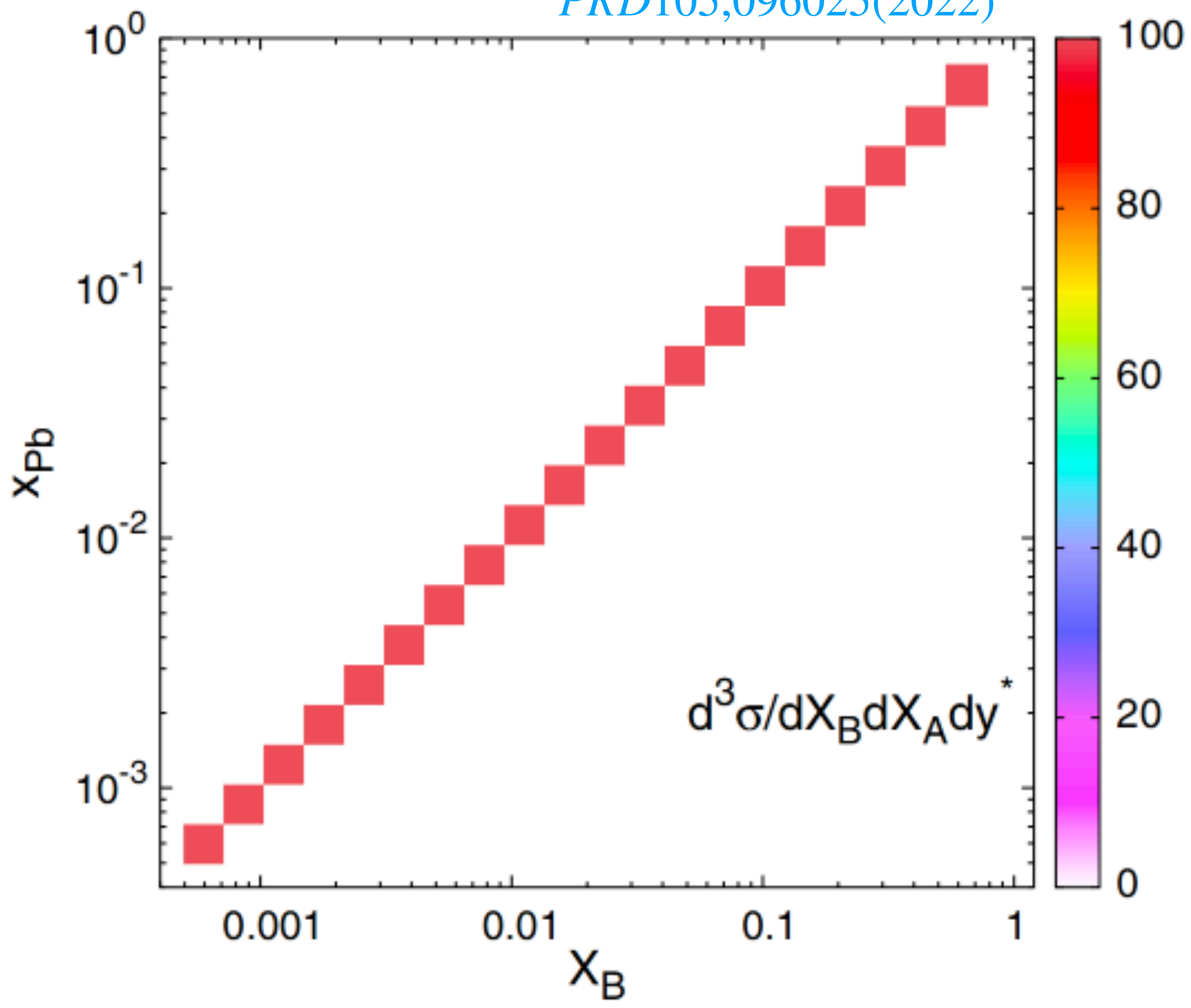

LO: $X_A = \mathrm{x_p}$ control the probe

$X_B = \mathrm{x_{Pb}}$ scan the target

Construction of the image of $r_i^A(x, Q^2)$ in pA

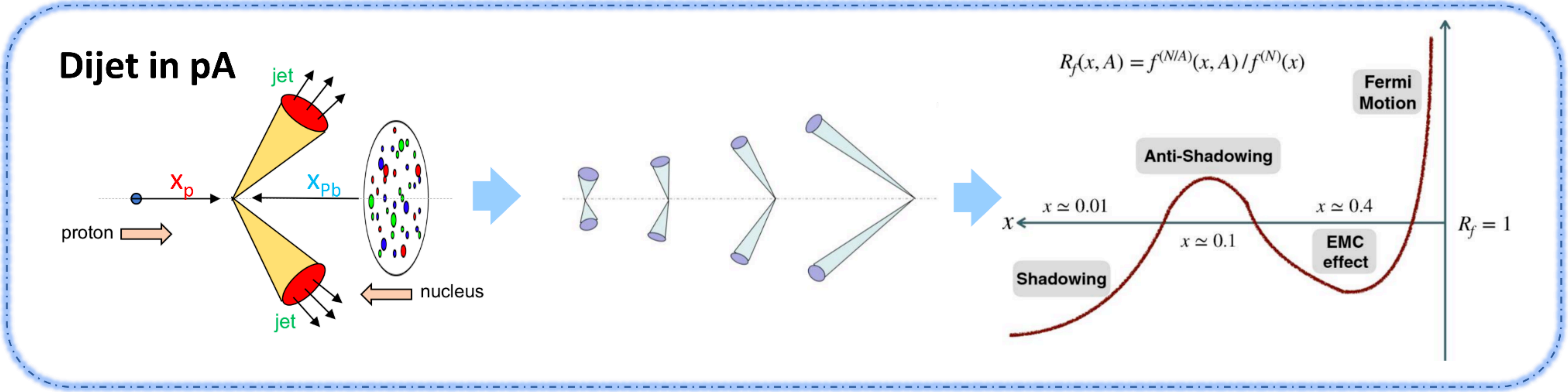

Shen, Ru, Zhang, PRD 105, 096025 (2022)

More advantages in pPb collisions

$$R_{pA}(v_1,v_2,v_3) \approx \frac{\sum_{a,b} f_a^p(x_a,\mu^2)\boxed{f_b^A(x_b,\mu^2)}H_{ab}(v_1,v_2,v_3)}{\sum_{a,b} f_a^p(x_a,\mu^2)\boxed{f_b^p(x_b,\mu^2)}H_{ab}(v_1,v_2,v_3)}$$

$\mathbf{r_i^A(x, Q^2)}$

1. Uncertainties from proton PDFs reduced.
2. Uncertainties from high-order corrections reduced.
3. Incoming from one side.
4. Experimental uncertainties also reduced.

Construction of the image of $r_i^A(x, Q^2)$ in pA

Extended to cases with fixed probing scales. $V^{(3)} = \{X_B, E^{JJ}, p_{T,avg}\}$

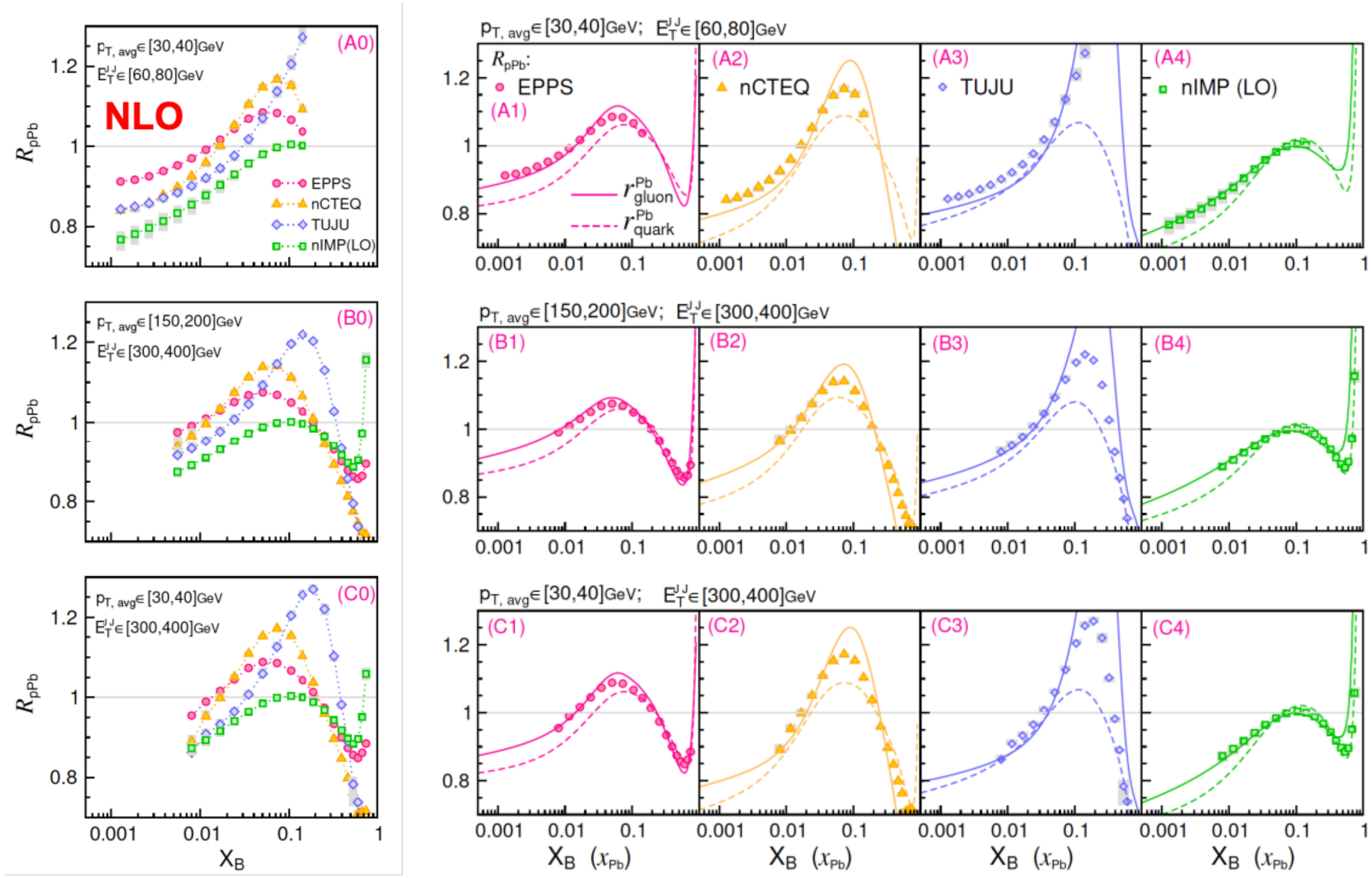

*PRD*105,096025(2022)

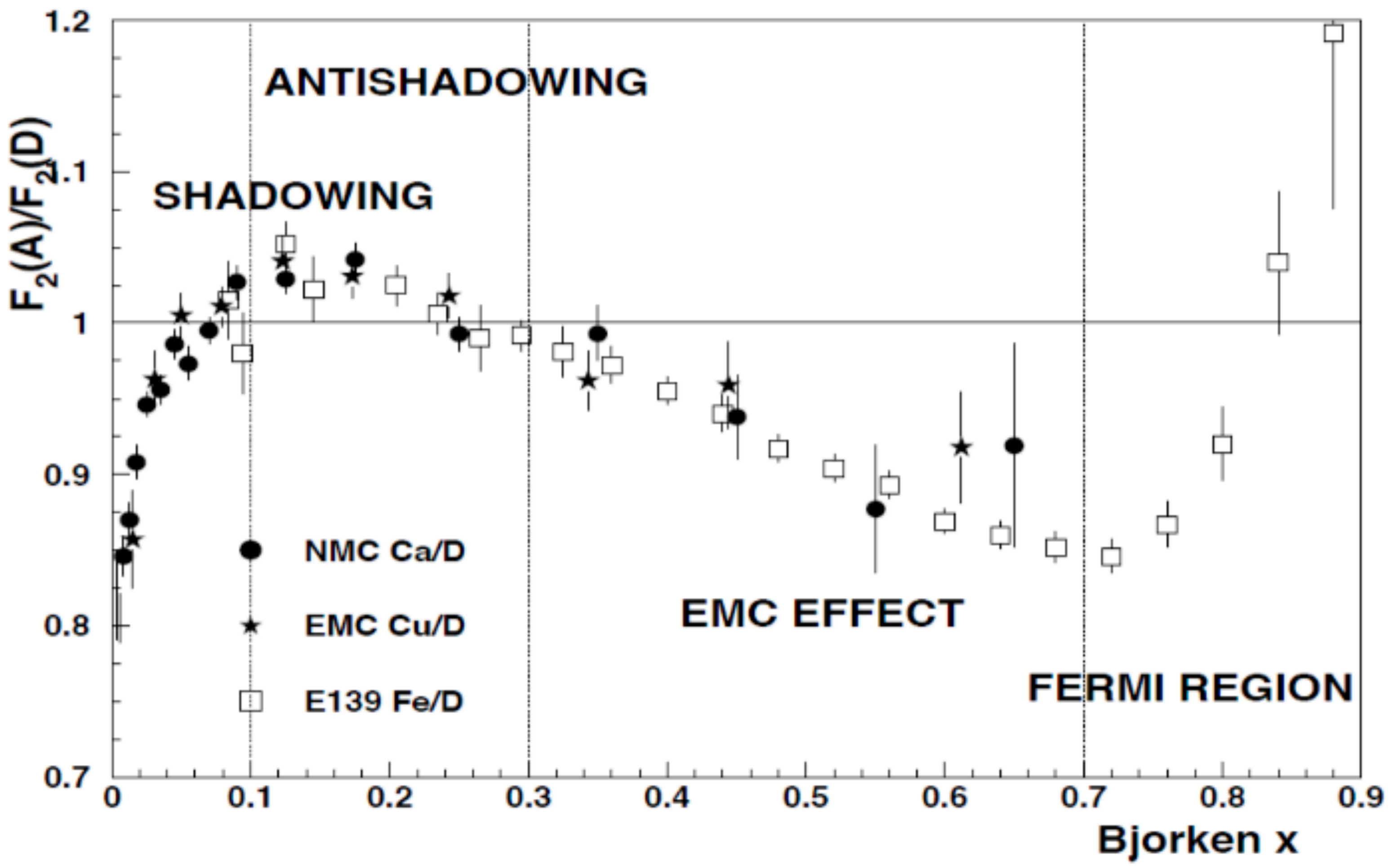

1. Scanning of $r_i^A(x, Q^2)$ in pA, verified at NLO.

2. An analogy to the image in DIS.

3. However, parton flavors are still mixed.

Construction of the image of $r_i^A(x, Q^2)$ in pA

Can parton flavors be further separated?

Multiprocess imaging based on the scanning with (x, Q^2)

Process	Partonic subprocess at LO
Z-boson	$q + \bar{q} \to Z \to l^+ l^-$
$Z + \text{jet}$	$q + \bar{q} \to Z + g$ $q(\bar{q}) + g \to Z + q(\bar{q})$
$Z + c\text{-jet}$	$c(\bar{c}) + g \to Z + c(\bar{c})$

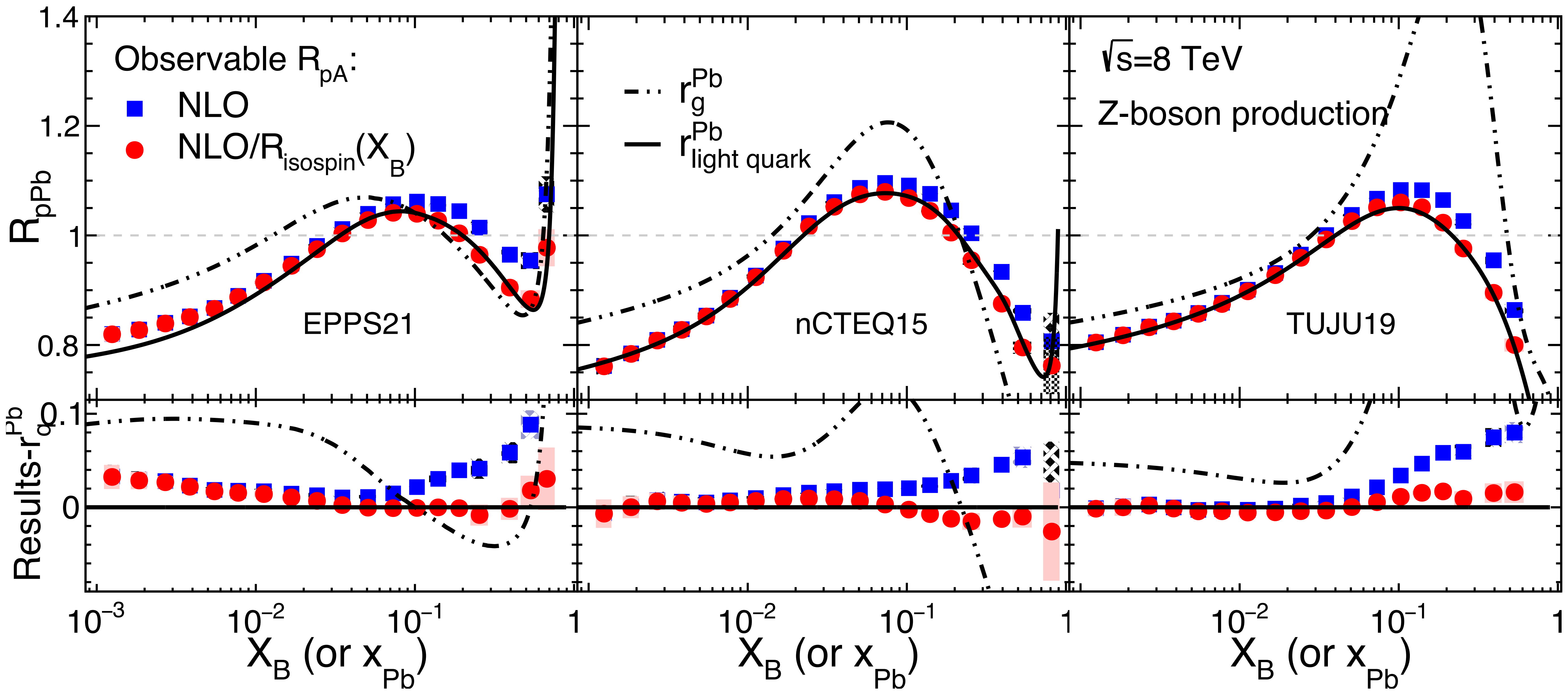

R_{pA} **for Z-boson productions nicely images the** $r_i^A(x, Q^2)$ **for light quarks!**

Construction of the image of $r_i^A(x, Q^2)$ in pA

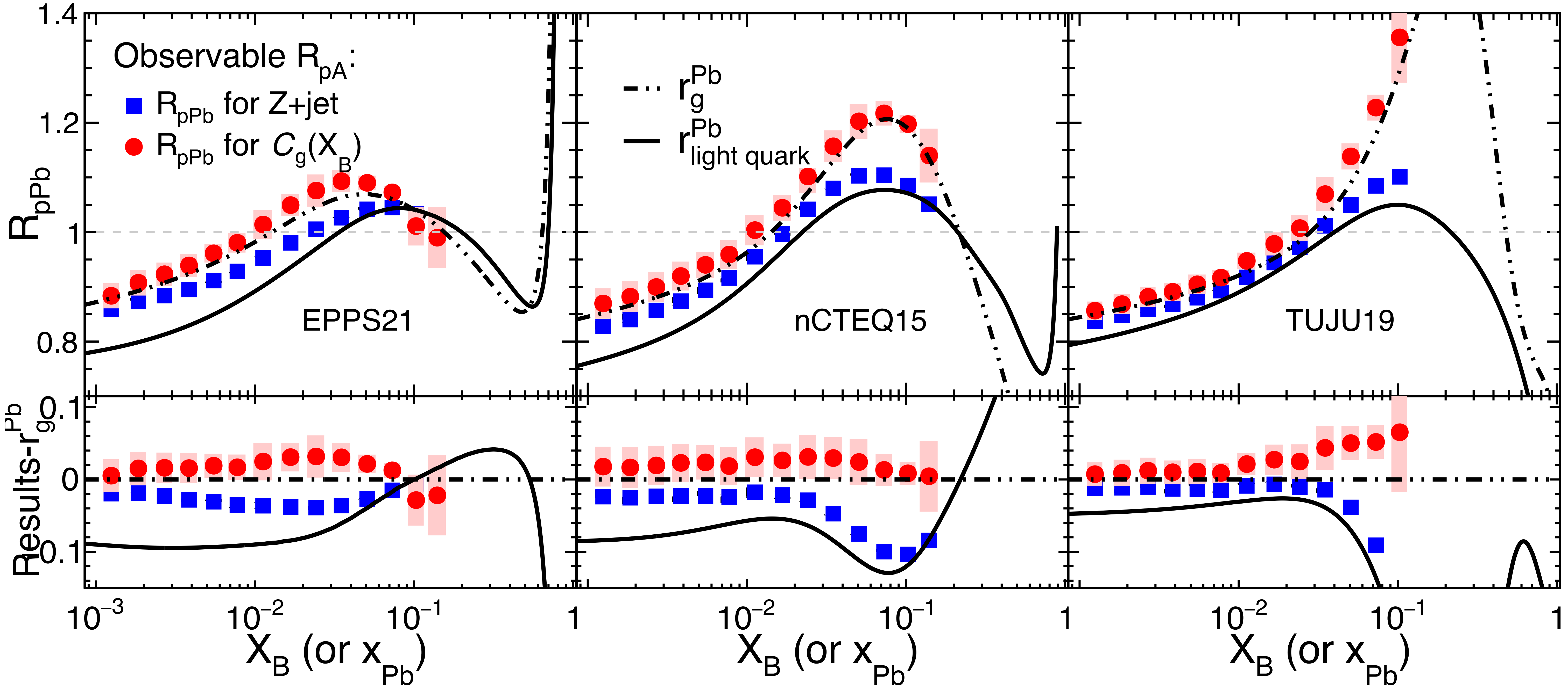

R_{pA} **for Z+jet productions images the mixture of** $r_i^A(x, Q^2)$ **for light quarks and gluons.**

A combined observable with Z-boson and Z+jet productions:

$$C_g(X_B) = \kappa_1(X_B) \times d\sigma^{Z+\text{jet}}(X_B) - d\sigma^Z(X_B), \qquad \kappa_1(X_B) = \frac{d\sigma^Z(X_B)}{[d\sigma^{Z+\text{jet}}(X_B)]_{\text{nuclear quark}}}$$

which suppress the effects from nuclear quarks and nicely images the $r_i^A(x, Q^2)$ **for gluons.**

Construction of the image of $r_i^A(x, Q^2)$ in pA

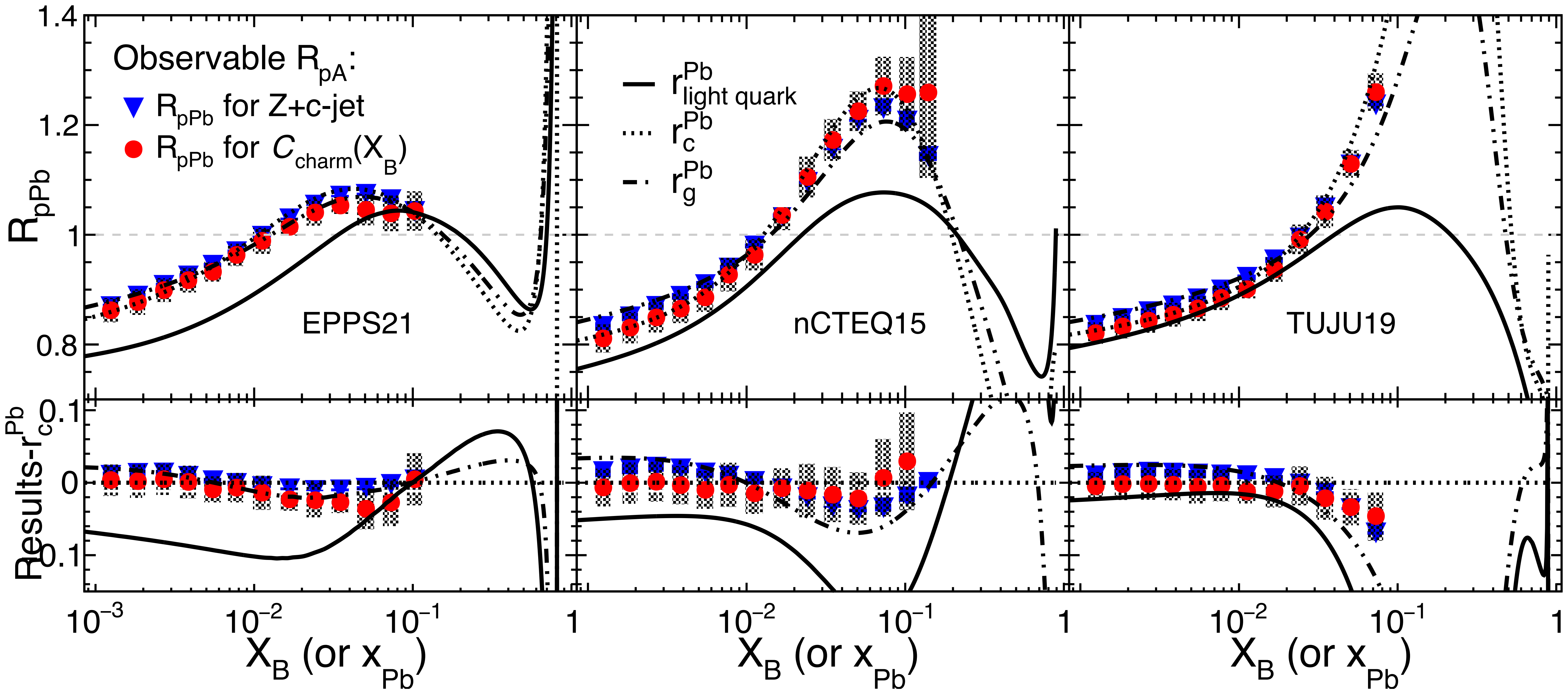

R_{pA} for Z+c-jet productions images the mixture of $r_i^A(x, Q^2)$ for charm quarks and gluons.

A combined observable with Z-boson, Z+jet and Z+c-jet productions:

$$C_{\text{charm}}(X_B) = \kappa_2(X_B) \times d\sigma^{Z+c\text{-jet}}(X_B) - C_g(X_B), \quad \kappa_2(X_B) = \frac{C_g(X_B)}{[d\sigma^{Z+c\text{-jet}}(X_B)]_{\text{nuclear gluon}}}$$

which nicely images the $r_i^A(x, Q^2)$ for charm quarks.

Construction of the image of $r_i^A(x, Q^2)$ in pA

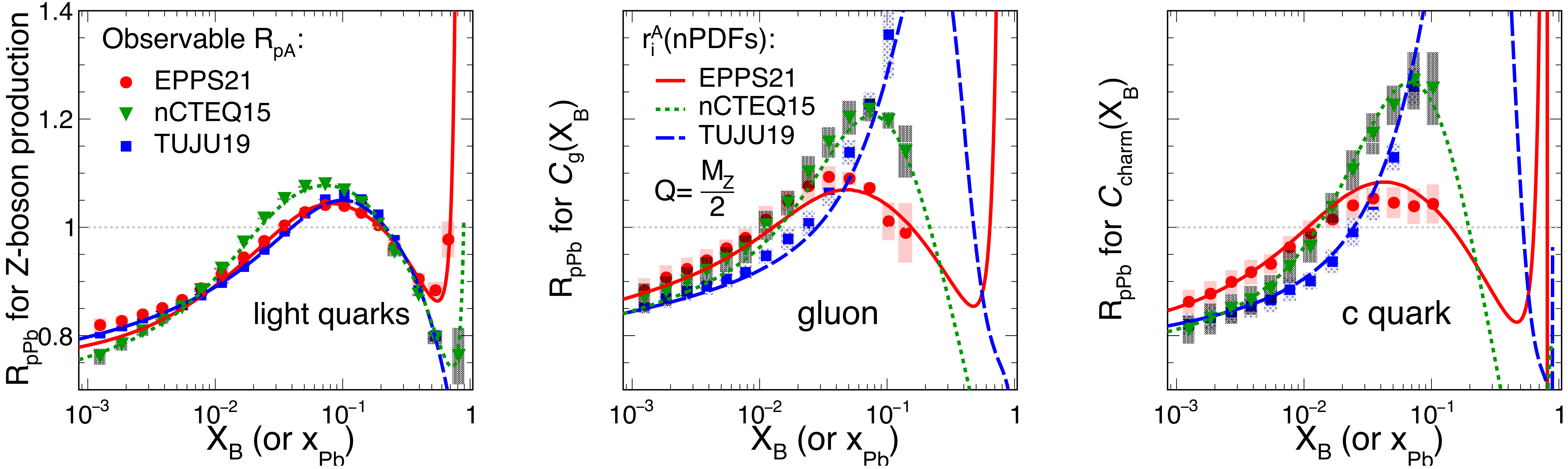

The results show the probability to separately image the $r_i^A(x, Q^2)$ for certain parton flavors at LHC.

Summary

- **An imaging methodology is developed to optimize the future measurements at LHC.**

  With better disentangled contributions of (x, Q^2, i) *for* $r_i^A(x, Q^2)$, *facilitate more efficient global analysis .*

- **Neither PDFs nor $r_i^A(x, Q^2)$ is directly measurable.**

  Compared to traditional observables, the proposed imaging observables provide somewhat preprocessed data with theoretical guidance.

- **Future applications:**

Other processes at the LHC

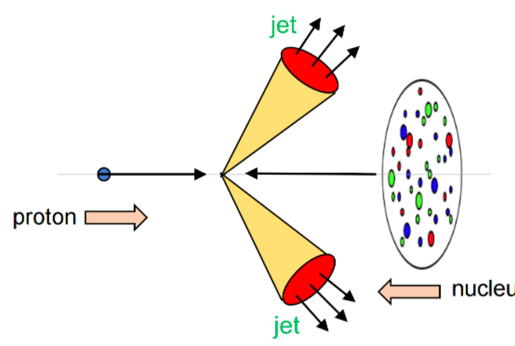

Dijet, Drell-Yan, γ-jet, ……

Combined study of LHC and EicC/EIC

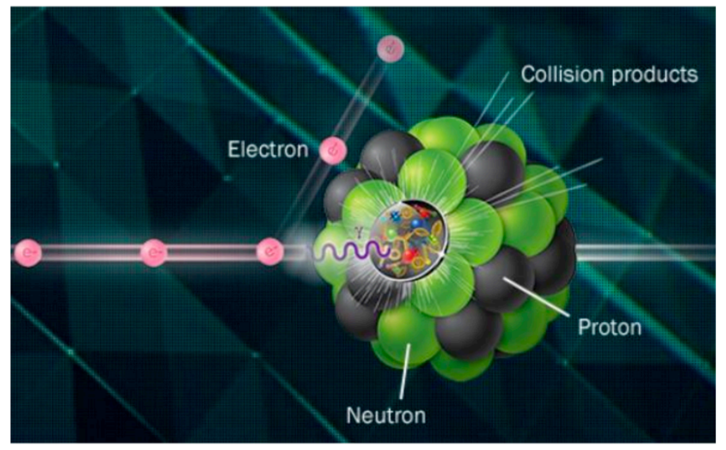

Systematic comparison spanning from pA to eA

Nuclear effects at higher-twist

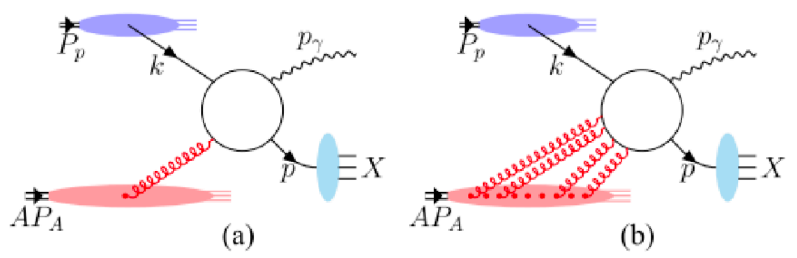

Fu, Kang, Salazar, Wang, Xing
PRL 135, 032301 (2025)